

Fast and Accurate Computation of Flux Density Formed by Solar Concentrators and Heliostats

François Hénault ¹, Gilles Flamant ², and Cyril Caliot ³

¹ Institut de Planétologie et d'Astrophysique de Grenoble, Université Grenoble-Alpes, France

² PROMES, CNRS, UPVD, France

³ CNRS, UPPA, E2S, LMAP, France

* Correspondence: François Hénault, henaultfbm@gmail.com

Abstract. Computing the flux densities provided by solar concentrators or focusing heliostats can be done in two different ways: A grid ray-tracing (GRT) procedure that makes use of a large number of ray bundles, starting from the solar disk and finally impinging the focal plane of the concentrator. The method is reliable and accurate, but requires extensive computing times. Alternatively, the flux densities can be estimated by using convolution algorithms. This latter method requires much less computing time, but is known to be less accurate when the incidence angle of the sunrays on the reflector increases. The objective of this contribution is to define an algorithm based on convolution products and fast Fourier transforms having high accuracy. The results show that RMS error differences between both models are typically lower than 1%.

Keywords: Solar Concentrator, Heliostat, Flux Density, Ray Tracing, Optimization

1. Introduction

Computing the flux densities provided by solar concentrators is a fundamental tool for optimizing the geometrical parameters of the facility. This contribution mainly deals with the concentrating power of focusing heliostats implemented in a solar tower power plant, but can be generalized to any other type of solar concentrator. Such numerical computations can be performed in two different ways, both described in Ref. [1]:- A ray-tracing model based on grid ray-tracing (GRT), starting from the solar disk, impinging the surface of the solar concentrator, and finally reaching the focal plane of the installation. This method is reliable and accurate, but requires extensive computing times.

- Alternatively, the flux density can be estimated by using convolution algorithms. This requires much less computing time, but is known to be less accurate when the incidence angle of sunrays at the heliostats increases [2].

The purpose of this communication is to define an algorithm based on a convolution model and fast Fourier transforms (FFT) algorithm having accuracy comparable to those of GRT models (section 2). Numerical results are given in section 3, before a brief conclusion is drawn in section 4.

2. Improved convolution model

2.1 Solar tower plant configuration

Let us consider the case of a solar tower power plant whose general configuration is depicted in Figure 1-A. Two main coordinate systems are defined:

- The X'Y'Z' reference frame attached to the solar receiver with X'-axis directed from South to North, Y'-axis from East to West, and Z'-axis from Nadir to Zenith,
- The XYZ reference frame attached to an individual heliostat with X its optical axis and YZ the lateral dimensions along which its geometry is defined (see Figure 1-B and Table 1).
- In the X'Y'Z' reference frame are defined three vectors (see Figure 1-A):
- **S** is a unitary vector directed to the centre of the moving Sun,
- **R** is the unitary target vector directed from the heliostat centre to the solar receiver centre,
- **N** is the bisecting vector between both previous ones.

The vectors **S**, **R** and **N** obey the Snell-Descartes law for reflection that writes in vectorial form as [3]:

$$\mathbf{S} + \mathbf{R} = 2(\mathbf{S} \cdot \mathbf{N}) \mathbf{N} = 2\cos i \mathbf{N}. \quad (1)$$

The main parameters employed in this paper are summarized in Table 1. The case is inspired from the THEMIS solar tower plant built in Targasonne, France [4] and its heliostat field: The considered heliostat is located at coordinates (86.6, 50., 0.) expressed in meters into the X'Y'Z' reference frame. It may be noted that the distance d from the heliostat to the solar receiver is kept equal to 100 meters and that the heliostat and the solar receiver are located at the same altitude along the Z'-axis, which is considered as the worst and most demanding case. The heliostat is made of $m \times n$ identical spherical modules of focal length f .

Table 1. Main parameters of the solar power plant and of the focusing heliostat.

Parameter	Symbol	Value	Unit
Target vector from heliostat to receiver	R	(86.6, 50., 0.)	m
Distance from heliostat to receiver	d	100	m
Incidence angle on solar receiver	β	30	degrees
Heliostat width along Y-axis	w	3.4	m
Heliostat height along Z-axis	h	3.	m
Number of heliostat modules	$m \times n$	4 x 2	
Modules width along Y-axis	w_M	0.7	m
Modules height along Z-axis	h_M	1.4	m
Modules focal length	f	$80 \leq f \leq 120$	m
Solar receiver diameter	d'	1.2	m

2.2 Double Fourier transform model

Most of convolution models developed so far are based on the "pinhole view" defined by F. Lipps in 1976 [5]. It states that the flux density distribution $I(x', y')$ formed by a heliostat at the solar receiver plane Y'Z' can be approximated as the convolution product of two functions $L(x', y')$ and $\text{PSF}(x', y')$:

$$I(x', y') = L(x', y') * \text{PSF}(x', y'), \quad (2)$$

where $L(x',y')$ is the ideal geometrical image of the Sun disk projected onto the solar receiver plane $Y'Z'$ and $PSF(x',y')$ is the Point spread function of the heliostat, i.e. the image that would be observed at the solar receiver if the Sun was reduced to a null or negligible angular diameter. Here the mathematical symbol $*$ denotes a convolution product.

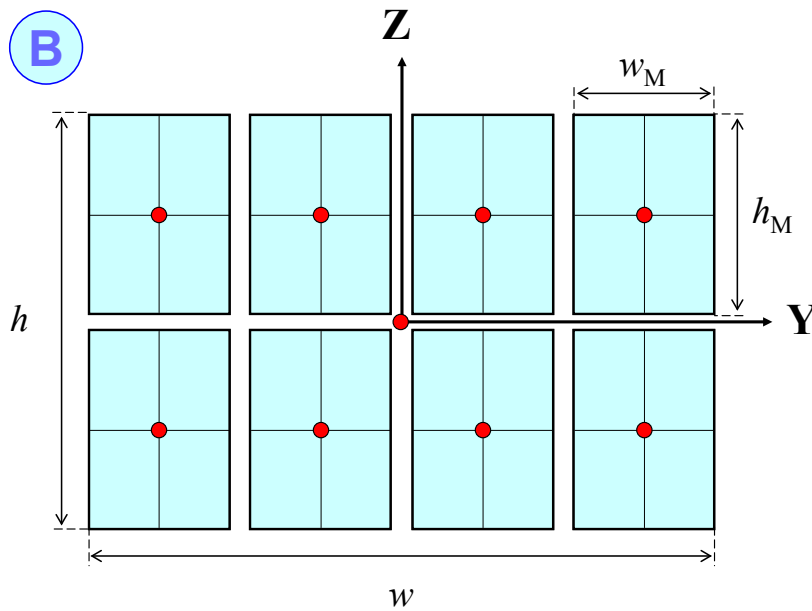
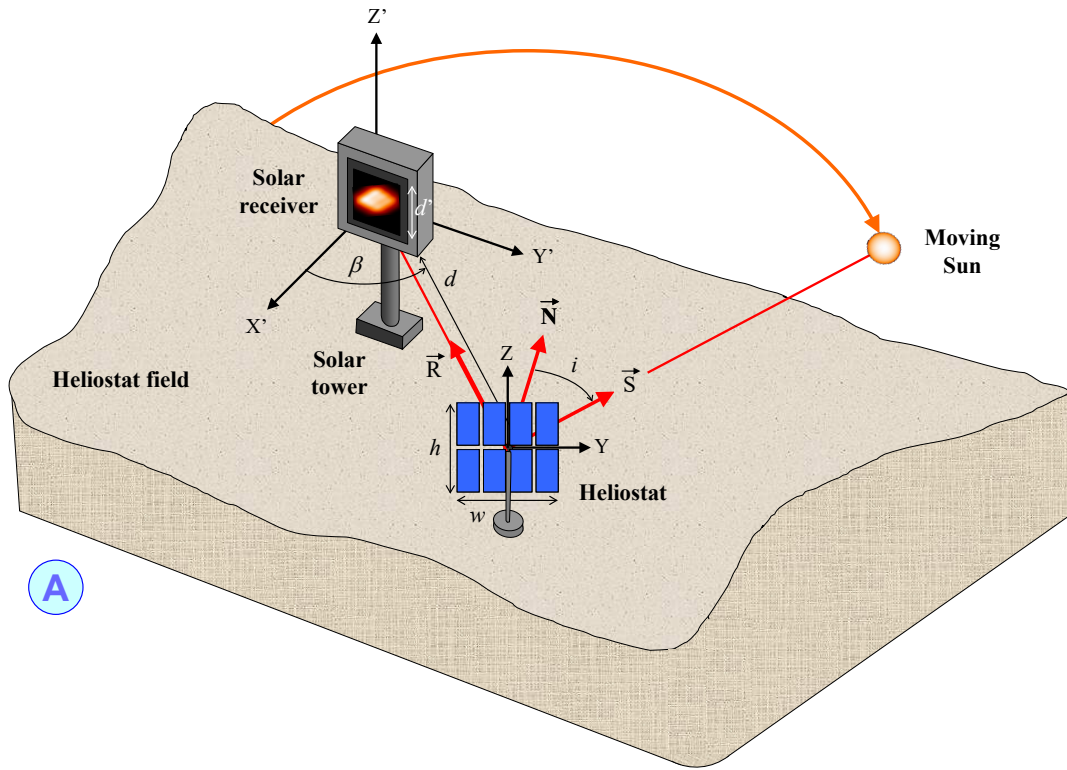


Figure 1. Solar tower power plant configuration (A). The geometry of the heliostats is shown in the bottom scheme (B).

Most of the convolution models developed so far make use of analytical developments of the convolution product in Eq. 2, and take astigmatism and defocus aberrations into account [3-5]. They may also include some additional "cone error" functions describing the opto-mechanical defects of the heliostat [2, 6-8]. Alternatively, this convolution product can be calculated by means of a double Fourier transform algorithm, whose steps are illustrated in Figure 2 and are described below:

1. Start from an analytical expression of the Sun angular radiance law $L(\varepsilon)$. Herein was used the Jose's formula [9] that is:

$$L(\varepsilon) = L_0 \left(0.39 + 0.61 \sqrt{1 - (\varepsilon/\varepsilon_0)^2} \right) \quad \text{when } 0 \leq \varepsilon \leq \varepsilon_0 \text{ and:} \quad (3)$$

$$L(\varepsilon) = 0 \quad \text{otherwise,}$$

with ε the angle of the incident ray with respect to the Sun disk centre, and ε_0 the Sun angular radius taken equal to 4.65 mrad.

2. Define the ideal Sun image at the solar receiver plane Y'Z' from the previous radiance formula, after mapping it by the distance d and the cosine factor $1/\cos\beta$, resulting in the function $L(x',y')$.
3. Compute the Point spread function $PSF(x',y')$ of the heliostat using GRT ray-tracing.
4. Compute the Fourier transforms of both functions $L(x',y')$ and $PSF(x',y')$ by use of a FFT algorithm.
5. Multiply the Fourier transforms of $L(x',y')$ and $PSF(x',y')$ together.
6. Compute the inverse Fourier transform of the result with the inversed FFT algorithm to finally obtain the flux density map $I(x',y')$ at the solar receiver plane.

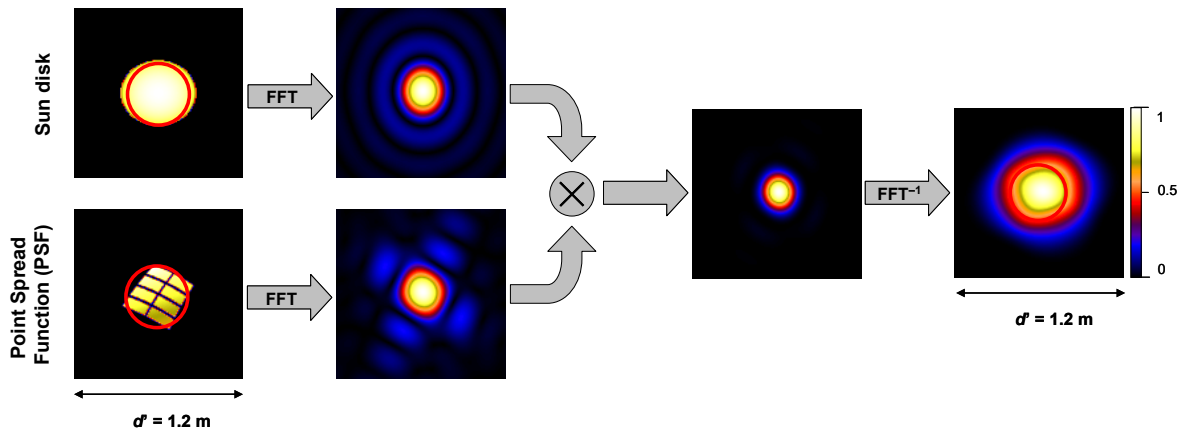


Figure 2. Illustrating the double Fourier transforms algorithm. Red circles indicate the diameter of the ideal image of the Sun.

The reason why this algorithm is much faster than any GRT model comes from the total number of launched rays. Assuming that both functions $L(x',y')$ and $PSF(x',y')$ are digitized into arrays of dimensions 64×64 and 128×128 at the Sun disk and heliostat respectively, GRT simulations involve $(64 \times 64) \times (128 \times 128) \approx 270.10^6$ rays traced one after the other. Conversely, the double FFT algorithm only uses grid ray-tracing for determining the function $PSF(x',y')$ formed by the "pinhole Sun". Assuming that it has smaller dimensions than the ideal Sun image, only a few sampling points are required to get a fair approximation of $PSF(x',y')$. Here the sampling number is set to 3×3 , therefore the number of traced rays reduces to $(3 \times 3) \times (128 \times 128) \approx 147500$. This allows a potential gain in computing time by a

factor about 450. Practically however, the computing time required by the three FFT operations is not negligible with respect to that needed by PSF ray-tracing. We finally found a gain in computing time about 250 with respect to the GRT model.

3. Numerical results

Numerical simulations were carried out with the IDL™ programming language in order to validate the double FFT algorithm and comparing it with the results of the GRT model. For both of them, two different cases were considered:

- Assuming that the latitude of the solar tower plant is 45 degrees, the heliostat described in Table 1 is set in Sun tracking mode from 09h00 to 15h00 GMT at the autumnal equinox day (case A).
- For the same heliostat at 15h00 GMT on the same day, different focal lengths are introduced on the spherical modules ($80 \leq f \leq 120$) in order to evidence the effect of the astigmatism and defocus aberrations (case B).

The numerical results are expressed in terms of Peak-to-Valley (PTV) and RMS differences between the flux density maps computed with both models, after normalizing their total power to unity. The flux density maps and their difference numbers are given in Table 1 and illustrated in the false colors views of Figure 2. The maximal PTV difference is about 7 %, and the RMS differences are always lower or equal than 1 %. Hence, we may conclude that the double Fourier transform model is validated at the price of a slightly lower accuracy that is compensated for by much faster computing times.

Table 2. Error differences between the GRT and improved convolution models for both cases (A) and (B).

<div style="text-align: center;"> A Spherical heliostat </div>		09-23-2022, Day time GMT				
		T = 09h00	T = 10h30	T = 12h00	T = 13h30	T = 15h00
PTV difference (%)		7,2	6,6	6,4	6,8	7,3
RMS difference (%)		0,8	0,9	0,9	1,0	0,8

<div style="text-align: center;"> B Spherical heliostat </div>		Heliostat modules focal length				
		$f = 80$ m	$f = 90$ m	$f = 100$ m	$f = 110$ m	$f = 120$ m
PTV difference (%)		5,0	6,3	7,3	6,7	5,8
RMS difference (%)		0,8	0,8	0,8	0,8	0,8

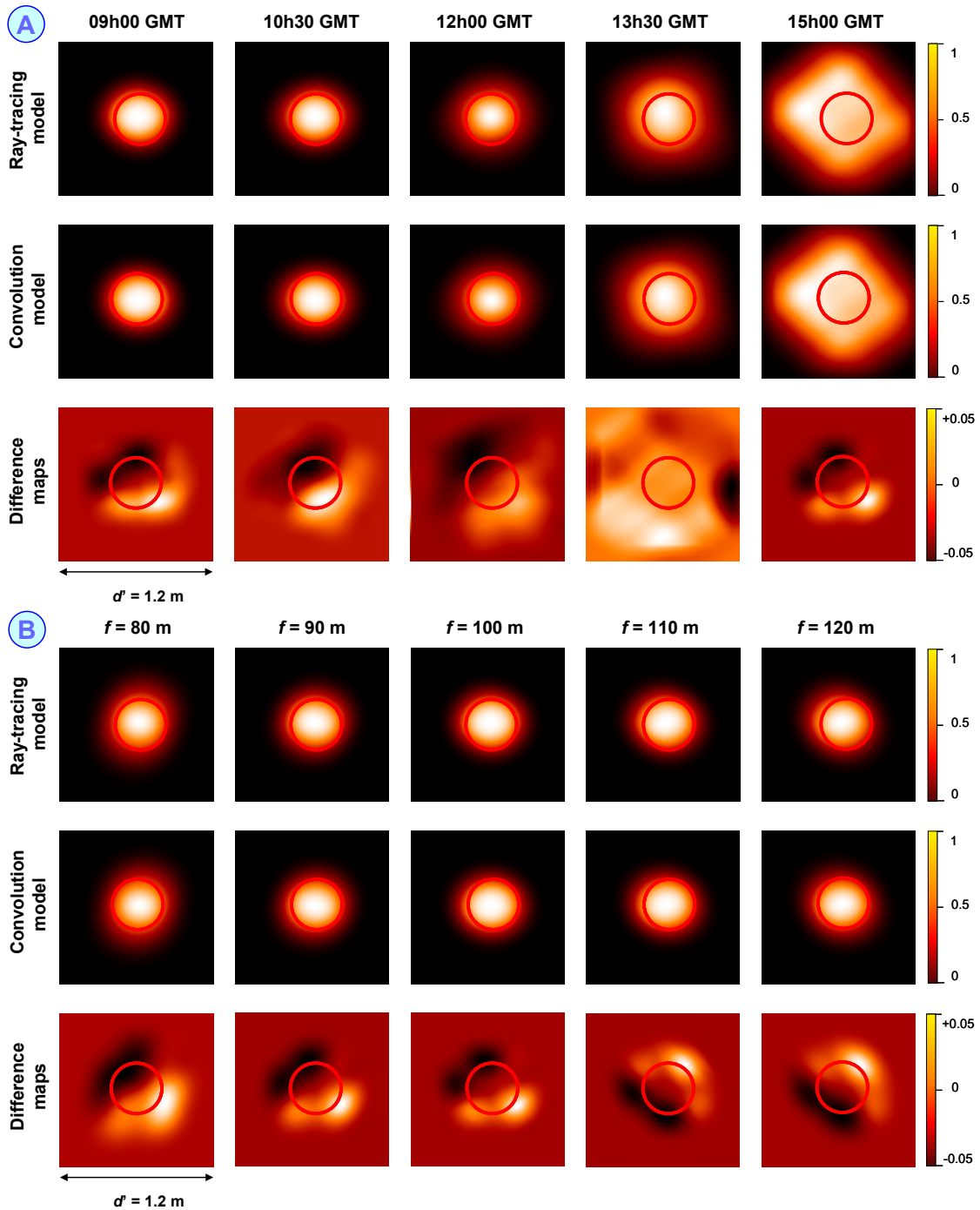


Figure 3. Sketch of flux density maps obtained for cases (A) and (B). For both cases the results computed with the GRT model are shown in the first rows and those from the improved convolution algorithm in the central rows. Difference maps are displayed at the bottom rows. All maps are shown in false color. Red circles indicate the diameter of the ideal Sun image at the focal plane.

4. Conclusion

This paper presents firstly an algorithm based on a convolution product and using Fast Fourier transforms for estimating the flux density formed by a solar concentrator. Numerical simulations are applied to the case of a Sun tracking focusing heliostat operating in a solar tower power plant. They demonstrate that the accuracy of this algorithm is comparable to those of classical grid ray-tracing models, since their RMS error difference is about 1% at most, even when the sunrays are impinging the heliostat under high incidence angles. The net gain factor in computing time with respect to GRT models is estimated around 250. This gain may be

further improved, either by more under-sampling the Point spread function of the heliostat, or by developing analytical expressions of the Fourier transform of the Sun disk, therefore reducing the number of required FFT from three to two. Finally, the double FFT algorithm may pave the way to fast and robust optimization of an entire heliostat field and of its pointing strategy.

Data availability statement

No data supporting the results of this contribution is available.

Author contributions

The authors confirm contribution to the paper as follows: Conceptualization, Formal analysis, Funding acquisition, Review & editing: F. Hénault, C. Caliot, G. Flamant. Methodology, Software, Validation, Visualization, Original draft: F. Hénault.

Competing interests

The authors declare that they have no competing interests.

References

- [1] P. Garcia, A. Ferrière, J.J. Bézian, "Codes for solar flux calculation dedicated to central receiver system applications: A comparative review," *Solar Energy* vol. 82, p. 189-197, 2008, doi: <https://doi.org/10.1016/j.solener.2007.08.004>.
- [2] Alberto Sánchez-González, "Analytic function for heliostat flux mapping with astigmatism and defocus," *Solar Energy* vol. 241, p. 24-38, 2022, doi: <https://doi.org/10.1016/j.solener.2022.05.045>.
- [3] M. Coquand, F. Hénault, C. Caliot, "Backward-gazing method for measuring solar concentrators shape errors," *Applied Optics* vol. 56, p. 2029-2037, 2017, doi: <https://doi.org/10.1364/AO.56.002029>.
- [4] B. Bonduelle, B. Rivoire, A. Ferriere, "La centrale expérimentale Thémis: bilan et perspectives," *Revue de Physique Appliquée* vol. 24, p. 453-461, 1989, doi: [10.1051/rphysap:01989002404045300](https://doi.org/10.1051/rphysap:01989002404045300).
- [5] F. Lipps, "Four different views of the heliostat flux density integral," *Solar Energy* vol. 8, p. 555-560, 1976, doi: [https://doi.org/10.1016/0038-092X\(76\)90075-X](https://doi.org/10.1016/0038-092X(76)90075-X).
- [6] F. J. Collado, "One-point fitting of the flux density produced by a heliostat," *Solar Energy* vol. 84, p. 673-684, 2010, doi: <https://doi.org/10.1016/j.solener.2010.01.019>.
- [7] A. Salomé, F. Chhel, G. Flamant, A. Ferrière, F. Thiery, "Control of the flux distribution on a solar tower receiver using an optimized aiming point strategy: Application to THEMIS solar tower," *Solar Energy* vol. 94, p. 352-366, 2013, doi: <https://doi.org/10.1016/j.solener.2013.02.025>.
- [8] F. Hénault, "Fast computation of solar concentrating ratio in presence of opto-mechanical errors," *Solar Energy* vol. 112, p. 183-193, 2015, doi: <https://doi.org/10.1016/j.solener.2014.12.002>.
- [9] P. Jose, "The flux through the focal spot of a solar furnace," *Solar Energy* vol. 1, p. 19-22, 1957, doi: [https://doi.org/10.1016/0038-092X\(57\)90167-6](https://doi.org/10.1016/0038-092X(57)90167-6).